

## On the phytoplankton bloom in coastal waters of southern King George Island (Antarctica) in January 2010: An exceptional feature?

I. R. Schloss,<sup>1,2,3,\*</sup> A. Wasilowska,<sup>4</sup> D. Dumont,<sup>3</sup> G. O. Almandoz,<sup>2,5</sup> M. P. Hernando,<sup>6</sup> C.-A. Michaud-Tremblay,<sup>3</sup> L. Saravia,<sup>7</sup> M. Rzepecki,<sup>8</sup> P. Monien,<sup>9</sup> D. Monien,<sup>9</sup> E. E. Kopczyńska,<sup>10</sup> A. V. Bers,<sup>11,a</sup> and G. A. Ferreyra<sup>3</sup>

<sup>1</sup> Instituto Antártico Argentino, Ciudad de Buenos Aires, Argentina

<sup>2</sup> Consejo Nacional de Investigaciones Científicas y Técnicas, Ciudad de Buenos Aires, Argentina

<sup>3</sup> Institut des sciences de la mer de Rimouski, Université du Québec à Rimouski, Rimouski, Canada

<sup>4</sup> Warsaw University, Faculty of Geology, Warsaw, Poland

<sup>5</sup> División Ficología, Facultad de Ciencias Naturales y Museo, Universidad Nacional de La Plata, La Plata, Argentina

<sup>6</sup> Comisión Nacional de Energía Atómica, San Martín, Buenos Aires, Argentina

<sup>7</sup> Área Biología y Bioinformática, Instituto de Ciencias, Universidad Nacional de General Sarmiento, Los Polvorines, Buenos Aires Argentina

<sup>8</sup> Nencki Institute of Experimental Biology, Polish Academy of Sciences, Warsaw, Poland

<sup>9</sup> Institute for Chemistry and Biology of the Marine Environment, Carl-von-Ossietzky University Oldenburg, Oldenburg, Germany

<sup>10</sup> Institute of Biochemistry and Biophysics, Polish Academy of Science, Department of Antarctic Biology, Warsaw, Poland

<sup>11</sup> Alfred-Wegener-Institute for Polar and Marine Research, Bremerhaven, Germany

### Abstract

Since the early 1990s, phytoplankton has been studied and monitored in Potter Cove (PC) and Admiralty Bay (AB), King George/25 de Mayo Island (KGI), South Shetlands. Phytoplankton biomass is typically low compared to other Antarctic shelf environments, with average spring–summer values below 1 mg chlorophyll *a* (Chl *a*) m<sup>-3</sup>. The physical conditions in the area (reduced irradiance induced by particles originated from the land, intense winds) limit the coastal productivity at KGI, as a result of shallow Sverdrup's critical depths ( $Z_c$ ) and large turbulent mixing depths ( $Z_t$ ). In January 2010 a large phytoplankton bloom with a maximum of around 20 mg Chl *a* m<sup>-3</sup>, and monthly averages of 4 (PC) and 6 (AB) mg Chl *a* m<sup>-3</sup>, was observed in the area, making it by far the largest recorded bloom over the last 20 yr. Dominant phytoplankton species were the typical bloom-forming diatoms that are usually found in the western Antarctic Peninsula area. Anomalously cold air temperature and dominant winds from the eastern sector seem to explain adequate light:mixing environment. Local physical conditions were analyzed by means of the relationship between  $Z_c$  and  $Z_t$ , and conditions were found adequate for allowing phytoplankton development. However, a multiyear analysis indicates that these conditions may be necessary but not sufficient to guarantee phytoplankton accumulation. The relation between maximum Chl *a* values and air temperature suggests that bottom-up control would render such large blooms even less frequent in KGI under the warmer climate expected in the area during the second half of the present century.

The western Antarctic Peninsula (WAP) region is one of the most rapidly warming on earth since the last 50 yr (Turner et al. 2005). Significant interannual climate variability in sea ice extension and ocean surface temperatures along the WAP has been associated with the Southern Annular Mode (SAM) and the El Niño Southern Oscillation (ENSO; Meredith et al. 2008; Schloss et al. 2012). Climate warming is supposed to induce important changes in polar ecosystems, from microbial communities (Piquet et al. 2011) to apex predators' levels (Trathan et al. 2007). Phytoplankton is at the base of the food web so that changes affecting primary production dynamics affect organisms of higher trophic levels. These organisms, in turn, may also be affected by even small variations in water temperature (Clarke et al. 2007). Climate change appears to already have induced changes in phytoplankton biomass

and composition along the WAP (Montes-Hugo et al. 2009).

Contrasting with other areas in the WAP, which show strong spring–summer algal blooms (Holm-Hansen et al. 1989), phytoplankton in the South Shetland Islands rarely show chlorophyll *a* (Chl *a*) concentrations (a proxy for phytoplankton biomass) higher than 3 mg m<sup>-3</sup> (Hewes et al. 2009). At the southern coasts of King George/25 de Mayo Island (KGI), the largest of the South Shetland Islands, phytoplankton biomass is even lower. Average spring–summer values for the 1991–2009 period were below 2 mg Chl *a* m<sup>-3</sup>. Values ranged from 0 to 6.7 mg Chl *a* m<sup>-3</sup>, the highest value ever recorded during 19 yr (see Schloss et al. 2012 for a detailed description of Chl *a* variation). Physical conditions in the area, such as intense winds, solar irradiance reduced by particles originated from the land, and the presence of sea ice, explain these low values (Schloss et al. 2012).

Phytoplankton has been studied and monitored at KGI in the Potter Cove (PC) area, close to the Argentinean Carlini Station (formerly Jubany) since the early 1990s

\* Corresponding author: ischloss@dna.gov.ar

<sup>a</sup> Present address: Deutsche Gesellschaft für Internationale Zusammenarbeit (GIZ), Eschborn, Germany

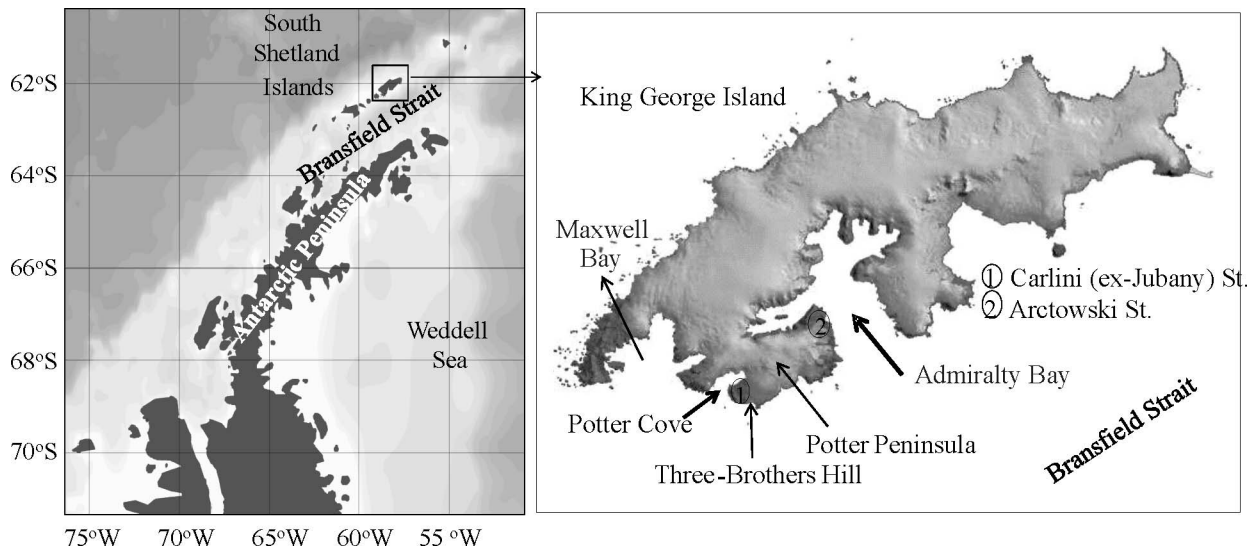


Fig. 1. Location of Arctowski and Carlini Stations, Admiralty Bay (AB) and Potter Cove (PC) in King George Island/25 de Mayo, South Shetland Islands.

(data available in doi:10.1594/PANGAEA.754676), and in the Admiralty Bay (AB) area since the 1980s by personnel of the Polish Arctowski Station (data available at doi:10.1594/PANGAEA.753936 and doi:10.1594/PANGAEA.754291). In January 2010, an anomalously large phytoplankton bloom was observed by both teams with a maximum of  $\sim 20 \text{ mg Chl } a \text{ m}^{-3}$  and monthly averages of 4 and 6  $\text{mg Chl } a \text{ m}^{-3}$  for PC and AB, respectively. In this paper, we present the main characteristics of this exceptional bloom and analyze the physical conditions that led to such high phytoplankton accumulation.

In previous attempts to understand phytoplankton dynamics in this area a conceptual model has been developed (Schloss et al. 2002), and threshold values for the average critical depth ( $Z_c$ , see below) and for the depth of turbulent mixing ( $Z_t$ , see below) were empirically determined in order to predict phytoplankton blooms (here defined as  $> 2 \text{ mg Chl } a \text{ m}^{-3}$ ) development from prevailing physical conditions in shallow coastal polar areas. In the present work, the same principles are applied to determine the relation between  $Z_c$  and  $Z_t$  and link it to the observed phytoplankton accumulation. However, instead of averaging field observations at a seasonal scale, the field data are used and analyzed at a 3 h to daily frequency. This improvement introduces time more explicitly as a key factor for phytoplankton accumulation. To further test the validity of this approach, the conditions during 11 austral spring–summer seasons from both AB and PC for which sufficient data are available, are analyzed.

## Methods

Results from two adjacent areas in southern KGI are presented here, namely from PC, close to the Argentinean Carlini Station, and AB, close to the Polish Arctowski Station (Fig. 1). Both areas are separated by the Potter Peninsula, which at its narrowest part is only  $\sim 5 \text{ km}$  wide. The peninsula presents a glacial landscape with abrasion

platforms offshore, which in parts are steep cliffs along the coast (Kraus et al. 2007), and a rather smooth interior. Its most prominent feature is the 196 m high Three Brothers Hill (Kraus et al. 2007). At its widest part, facing the Bransfield Strait, the Potter Peninsula is  $\sim 25 \text{ km}$  wide. Sampling sites at PC and AB are at a distance of 9 km from each other (see below); the main axis of PC has a northeast–southwest orientation, with the mouth opening into Maxwell Bay at the southwest, while the sampling area in AB has mainly an east–west orientation, with its mouth opening into the Bransfield Strait to the northeast (Fig. 1).

In January 2010, each site was sampled at three stations along a transect from the respective inner (coastal) to the outer areas. Although in previous studies in PC two of the sampling stations were usually analyzed separately, for the sake of the zonal analysis and the comparison between AB and PC, each set of values for the three stations will be averaged and merged into one single set at each site (PC and AB).

*Potter Cove*—PC is a small (7 km<sup>2</sup>), wide, and shallow bay. A transversal sill separates it into an inner ( $< 50 \text{ m}$  water depth) and an outer cove ( $\sim 100 \text{ m}$  water depth). The circulation in PC is strongly influenced by the general cyclonic circulation of the adjacent Maxwell Bay that reaches down to 500 m depth (Schloss et al. 2002).

*Sampling:* Air temperature, wind speed and direction, and cloud cover were measured every 3 h by the Servicio Meteorológico Nacional of the Argentinean Air Force at Carlini–Jubany Station. Anomalies for January 2010 wind speed and air temperature were estimated as in Schloss et al. (2012). Air temperature data are presented either as absolute or average values and are also used to compute total and positive degree-days. Total degree-days is the sum of daily-averaged air temperature in degrees Celsius ( $^{\circ}\text{C}$ ), whereas positive degree-days is the sum of daily-averaged air temperatures above  $0^{\circ}\text{C}$  only. This has been calculated for the austral spring–summer season (November to

March). The oceanographic sampling was conducted at three stations on six occasions in January 2010. This sampling is part of a long-term monitoring program that started in 1991, during which the water column in PC is sampled weekly in summer and biweekly in winter, whenever the meteorological conditions allow it. A Sea-Bird SBE Conductivity–Temperature–Depth (CTD; Sea-Bird Electronics) was used to record seawater temperature and conductivity (transformed in salinity). Water samples were collected at five depths (i.e., 0, 5, 10, 20, and 30 m) with 4.7 liter Niskin bottles.

*Sample analyses:* For Chl *a* analysis, seawater (0.25–2 liters) was filtered onto 25 mm Whatman GF/F filters under gentle vacuum and dim light. Photosynthetic pigments were extracted in 90% acetone for 24 h at 4°C in the dark. Extract absorbance was read using a Shimadzu RF-1501 spectrophotometer, and concentrations were calculated and corrected for phaeopigment content following the method of Strickland and Parsons (1972). Total suspended particulate matter (TPM) concentration was measured gravimetrically after filtering 0.25–2 liters of seawater through combusted pre-weighed 25 mm Whatman GF/F filters. After filtration, filters were rinsed twice with distilled water in order to remove salts and then dried for 24 h at 60°C, and weighed again. Samples for nutrients were taken only after the bloom period (January 2010) at two sites (inner and outer cove). During summer 2011, six sites from the inner to the outer cove were sampled for nutrients. Immediately after sampling, seawater samples were filtered through 0.45  $\mu\text{m}$  polycarbonate syringe filters (Satorius), poisoned with  $\text{HgCl}_2$  (105  $\mu\text{g}$   $\text{HgCl}_2$   $\text{mL}^{-1}$  sample), and stored at 4°C until analysis. Nitrate ( $\text{NO}_3^-$ ) and phosphate ( $\text{PO}_4^{3-}$ ) were analyzed using a microtiter-plate reader (MultiScan GO, Thermo-Fischer) and miniaturized spectrophotometric methods modified after Miranda et al. (2001;  $\text{NO}_3^-$ ) and Laskov et al. (2007;  $\text{PO}_4^{3-}$ ). An exception to this are the samples taken during austral summer 2010–2011 where  $\text{PO}_4^{3-}$  was measured by continuous-flow spectrophotometry (Quattro, Seal Analytical) based on the method described in Quattro applications (Method No. Q-031-04 Rev.2). Macronutrient data were verified by measuring independent reference solutions; therefore, precision and accuracy can be stated as better than 0.53% and 4.9% for  $\text{NO}_3^-$  and 0.03% and 3.7% for  $\text{PO}_4^{3-}$  for both methods. Averages and standard deviations are presented.

*Phytoplankton analysis:* Subsamples for phytoplankton taxonomic analysis were further kept in dark bottles after fixation with 4% acidic Lugol and stored under cold conditions (4°C) until analysis. Subsurface qualitative phytoplankton samples were additionally taken using a 20  $\mu\text{m}$  mesh net, and fixed and stored as previously described. Qualitative samples were examined using phase-contrast, differential interference contrast, and ultraviolet epifluorescence microscopy under two Leica Model DM2500 microscopes. For diatom frustules observation, organic material was removed from net subsamples using sodium hypochlorite as described in Almandoz et al. (2011). Clean material was then mounted on permanent slides using Naphrax® (The Biology Shop). Further

scanning electron microscopy observations were made with a Low Vacuum Jeol JSM-6360.

For quantitative estimations, cells were enumerated with a phase-contrast Leica Model Digital Media & Innovation Lab light-emitting diode inverted microscope according to the procedures described by Utermöhl (1958). Subsamples of 50 or 100 mL were settled for 24 or 48 h, respectively, in a composite sedimentation chamber. At least 100 cells of the dominant taxa were counted in one or more strips of the chamber or random fields at 250 $\times$  or 400 $\times$ , depending on their concentration and size. The whole chamber bottom was also scanned at 100 $\times$  to count large and sparse species. Cell carbon content was estimated as in Almandoz et al. (2011).

*Admiralty Bay—AB* is the largest bay of the South Shetlands Islands, covering an area of 122 km<sup>2</sup>. It has the shape of a narrow fjord deeply incised into land. The central part of AB exceeds water depths of 530 m; the northern part is divided into three inlets where depths vary between 50 and 200 m. Water exchange with the adjacent Bransfield Strait is favored by wind-driven surface currents and tidal exchanges of deep-water masses (Pruszek 1980).

*Sampling:* Air temperature (average, maximum, and minimum values), wind speed and direction, and cloud cover data were taken daily at Arctowski Station using an automatic Davis Vantage pro 2 meteorological station. Water profiles were examined from a fishing boat at three stations three times a month throughout seasons 2009–2010 (from November 2009 to March 2010) with a Midas CTD multi-parameter profiler (Valeport) additionally equipped with a photosynthetically active radiation (PAR) irradiance meter and a Seapoint Turbidity sensor. Samples for pigment analysis were taken from the surface to a water depth of 100 m at 5 to 10 m intervals, and for microscopy analysis at 5, 20, and 40 m depth using 7.5 liter Niskin bottles and transferred into 2.5 liter opaque Nalgene bottles.

*Sample analyses:* Samples for pigment analysis were filtered immediately after collection through 45 mm Whatman GF/F filters under gentle vacuum and dim light. Filters were stored in a freezer at  $-70^\circ\text{C}$  until analysis within 1 week. The pigments were extracted in 3 mL of methanol by ultrasonication (2 min at 10 W, Omni-Ruptor 250) while kept on ice. Analyses were carried out in the laboratory at Arctowski Station using a Shimadzu high-performance liquid chromatography (HPLC) system equipped with an ultraviolet-visible (UV) and fluorescence detector on a Waters Spherisorb C<sub>18</sub> ODS2 column. Gradient method recommended by the Scientific Committee on Oceanic Research (Wright et al. 1991) was used to separate pigments. The pigments were identified by comparison of their retention times and absorption spectra with standards (DHI Laboratory products) and also with literature data (Jeffrey et al. 1997). Calibration curves were made using external standards. The purity of pigment standards was tested according to the procedure recommended by Mantoura and Repeta (1997). Recalibration of the chlorophyll area:concentration relationship in the HPLC system was performed on each day before starting

the sample analysis using readily available pigment standards (chlorophyll *a* and *b*). The variations of pigment response factor never exceeded 5%. Water samples for nitrate and phosphate analyses were filtered through a 45 mm Whatman GF/F filters and deep frozen ( $-80^{\circ}\text{C}$ ) at the Arctowski laboratory. Analyses were carried out in the home laboratory in Poland 60–90 d later, following standard analytical procedures (Grasshoff et al. 1999) and using a Shimadzu UV-160A spectrophotometer. Comparison of commonly used photometric methods and miniaturized spectrophotometries are described in Miranda et al. (2001) and Laskov et al. (2007).

**Phytoplankton analysis:** For microscopic examination and cell counting, aliquots of 100 mL were preserved with glutaraldehyde–Lugol solution at a final concentration of 1% and stored in the dark at  $4^{\circ}\text{C}$  until analysis. Algal cells were counted at  $400\times$  magnification with a Nikon inverted microscope according to the procedures described by Utermöhl (1958). At least 300 cells were included in the counts of every sample.

**Physical–biological model and data analysis**—The conceptual model proposed by Schloss et al. (2002) attempted to determine the environmental threshold values for the factors controlling phytoplankton accumulation in Antarctic shelf zones. The model is based on Sverdrup's (1953) hypothesis saying that there exists a compensation depth, noted  $Z_c$ , at which the vertically integrated production rate is balanced by respiration loss over a 24 h cycle. This depth is called the critical depth and defines a volume space in the ocean where light conditions are favorable for phytoplankton photosynthesis. It depends on irradiance in the water column, which varies with the time of the year, the latitude, the presence of sea ice, and the absorption or scattering by dissolved organic and particulate matter in the water column (Schloss et al. 2002). Sverdrup's critical depth (m) can be calculated after the formula from Nelson and Smith (1991) as:

$$Z_c = \frac{0.8 \int_0^T E_0 dt}{TE_n K_d} \quad (1)$$

where  $E_0$  is the net downward surface irradiance in  $\text{W m}^{-2}$ ;  $T = 24$  h is the integration period; 0.8 is an adimensional surface reflectance correction factor for global PAR and near-surface absorbance of wavelengths larger than 650 nm (Nelson and Smith 1991);  $E_n$  is the photo-compensation irradiance, here considered as  $7.81 \text{ W m}^{-2}$ , obtained experimentally for PC by Schloss and Ferreyra (2002), which is close to the value of  $7.27 \text{ W m}^{-2}$  proposed by Nelson and Smith (1991); and  $K_d$  is the diffuse attenuation coefficient. Here only PAR attenuation is considered since UV is highly absorbed between 0–5 m depth in these coastal waters (Hernando and Ferreyra 2005).  $K_d$  was determined by using an empirical relation involving the TPM concentration in PC after Schloss and Ferreyra (2002) and by the Beer–Lambert's Law applied to PAR data in AB. The large amount of particles present in surface waters in PC prevented the direct use of Lambert's Law in that area (Schloss and Ferreyra 2002).

Turbulence is the second factor considered by Schloss et al. (2002). It determines how phytoplankton cells move vertically in the water column and how far down they are likely to be transported as they are being swirled around by a cascade of turbulent overturning eddies. The trajectory of one phytoplankton cell is random and unpredictable, but the vertical scale over which the cell will likely travel can be estimated according to Denman and Gargett (1983):

$$Z_t = \sqrt{2K_z t} \quad (2)$$

which corresponds to the Lagrangian root mean square vertical displacement of neutrally buoyant particles in coastal stratified waters submitted to wind stress. Here,  $t$  is the duration of a wind event,  $K_z = 0.25N^{-2}\varepsilon$  is the vertical eddy diffusivity,  $N^2 = g\rho^{-1}(\partial\rho/\partial z)$  is the squared Brunt–Väisälä frequency with  $\rho$  being the seawater density,  $g$  the gravitational acceleration, and  $\varepsilon$  the dissipation rate of turbulent kinetic energy due to winds given by

$$\varepsilon = \frac{\rho_a C_{10}}{\rho_w H} K_w U_{10}^3 \quad (3)$$

where  $C_{10}$  is the air drag coefficient,  $\rho_a$  and  $\rho_w$  are the air and water density, respectively,  $H$  is the depth of the water column (100 m for the average sampling station at PC and 150 m for AB),  $K_w = 4 \times 10^{-2}$  is a correction factor for the wind at surface (Denman and Gargett 1983), and  $U_{10}$  is the wind speed at 10 m above sea level. The air drag coefficient formulation is the one from Yelland and Taylor (1996) and is a nonlinear function of the wind speed. Given  $U_{10}$  from a meteorological station and  $N^2$  from in situ CTD data at a given time, only  $t$  must be set in order to obtain a value for  $Z_t$ . Here we choose to evaluate  $Z_t$  for two time intervals, namely  $t = 3$  h, corresponding to the highest frequency for which wind data are available, and  $t = 24$  h, which is among the highest doubling rates measured for Antarctic phytoplankton (Spies 1987). We believe these two values give a conservative estimate of  $Z_t$  given the high degree of uncertainty. For PC, 3 h wind speed data were averaged over the interval of interest before calculating  $Z_t$ . For AB only daily-averaged wind speeds were available; therefore, only this value was used to estimate  $Z_t$ . In order to limit  $Z_t$  from taking unrealistically large values,  $Z_t$  obtained from Eq. 2 was compared and limited to the buoyancy depth scale  $Z_b = \varepsilon^{1/2}N^{-3/2}$ , representing the scale of the largest eddies possible in a stratified fluid (Denman and Gargett 1983). Extreme values of  $Z_t$  were finally used to determine an interval for the most likely Lagrangian vertical extent due to the direct action of the wind. By comparing these two characteristic depths,  $Z_t$  and  $Z_c$ , the Sverdrup's concept can be further translated by stating that phytoplankton accumulation is possible if the condition  $Z_c > Z_t$  is maintained for a certain period to allow for the effective growth and accumulation of phytoplankton. This approach was applied to study the physical environment in both regions and was further tested for one additional season, 2007, in AB and for 1992, 1996, 1999, 2001, 2008, 2009, and 2011 in PC. The validity of the model was statistically tested by means of a stepwise multiple regression, using Statistica software (StatSoft), and considering the  $Z_c:Z_t$

Table 1. Characteristics of air temperature, sea surface temperature (SST), sea surface salinity, nutrients, and total particulate matter (TPM) for Admiralty Bay (AB) and Potter Cove (PC). For PC, data from three of the 3 yr representing contrasting conditions after the formalization of the conceptual model are presented. Nutrients for year 2010 in PC correspond to the week after the blooming period, nd, no data.

	January	PC			AB
		2001	2010	2011	2010
Air temperature (°C)	Average	1.88	1.02	1.82	1.14
	Standard deviation	1.67	1.86	1.90	1.48
	Maximum	7.60	7.00	6.80	5.80
	Minimum	-1.40	-2.80	-3.00	-2.70
SST (°C)	Average	1.17	0.73	1.64	0.77
	Standard deviation	0.07	0.03	0.07	0.11
Salinity	Average	34.15	34.09	33.25	34.11
	Standard deviation	0.07	0.13	1.42	0.13
Nitrates ( $\mu\text{mol L}^{-1}$ )	Average	nd	26.00	23.00	16.00
	Standard deviation	nd	1.40	1.90	1.80
Phosphates ( $\mu\text{mol L}^{-1}$ )	Average	nd	2.40	1.80	4.40
	Standard deviation	nd	0.30	0.20	1.40
TPM ( $\text{mg m}^{-3}$ )	Average	3.35	7.20	11.40	nd
	Standard deviation	9.48	4.80	6.60	nd

ratio, the maximal duration of the condition  $Z_c:Z_t > 1$  (hereafter called “duration”) and air temperature (total degree-days) as independent variables and Chl *a* (after a square root transformation) as the dependent variable.

*ENSO and SAM data*—The SAM index according to Marshall (2003; <http://www.nerc-bas.ac.uk/icd/gjma/sam.html>) was used. This is an observation-based index, calculated as the difference of normalized monthly zonal six-station mean sea-level pressure values, estimated at 40°S and 65°S. Furthermore, the bivariate ENSO time series (BEST) index (Smith and Sardeshmukh 2000) was used, which includes some explicit atmospheric processes, following Meredith et al. (2008). Monthly values of the BEST index were obtained from the Climate Diagnostics Center of the National Oceanographic and Atmospheric Administration (data available at <http://www.cdc.noaa.gov/people/cathy.smith/best/>).

*Models of maximum Chl *a* concentrations based on environmental data*—An information-theoretic approach was additionally used to fit maximum spring–summer Chl *a* values (Chl*a*Max) measured in AB and PC, including all of the 22 seasons for which summer Chl *a* data were available for the 1991–2011 period to evaluate their relation to air temperature (as total degree-days, *Methods* section), and to ENSO and SAM indices. A thorough introduction to information-theoretic model selection is given in Burnham and Anderson (2002). Briefly, a set of possible models was tested and their plausibility analyzed in order to get the closest one to full reality. This approach is based on the calculation of the Akaike Information Criterion (AIC). Operationally, AIC are computed for each of the models and the model with the smallest AIC value is selected as the “best,” in the sense of information loss minimization (Burnham et al. 2011). Due to the small sample size of the data sets, we applied a second-order bias correction to AIC which is denoted by AICc.

To rank models we calculated differences in AICc as shown below:

$$\begin{aligned}\Delta_i &= \text{AICc}_i - \text{AICc}_{\min} \Delta_i \\ &= \text{AICc}_i - \text{AICc}_{\min} \quad (\text{for } i = 1, 2, \dots, N)\end{aligned}$$

where  $\text{AICc}_{\min}$  denotes the minimum of the  $\text{AICc}_i$  values for the  $N$  models defined. We also calculated the probability of each model given the data as specified by Burnham et al. (2011). After an exploratory analysis, the square root of Chl*a*Max was used as dependent variable in order to get a Gaussian distribution. To explore the possible functional relations between Chl*a*Max and the independent variables, univariate generalized additive models (Wood 2006) were used. Based on these results, a set of models was built using the three variables, the possible subsets of two variables, and only one variable. The models were fitted using generalized least squares with the nlme library of the R statistical software version 3.1-106, which allows fitting the models with an auto-correlated error structure. (The R script and raw data used are available at <http://dx.doi.org/10.6084/m9.figshare.153954>.)

## Results

*Environmental data*—No significant differences in air temperature were evident between AB and PC. During January 2010 (Table 1) air temperature averages were  $1.0 \pm 1.9^\circ\text{C}$  in PC and  $1.1 \pm 1.5^\circ\text{C}$  in AB (Kolmogorov–Smirnov test,  $p > 0.1$ ). A few days prior to the observed phytoplankton bloom (from 20 December 2009 to 15 January 2010) temperatures were  $0.8 \pm 1.6^\circ\text{C}$  considering data from both places. For the sake of comparison with long-term data, in PC average air temperature during January for the 1991–2009 period was  $2.5 \pm 0.5^\circ\text{C}$  (Fig. 2a). Temperature anomaly (Schloss et al. 2012) was  $-1.5^\circ\text{C}$  for January 2010, but also negative for November

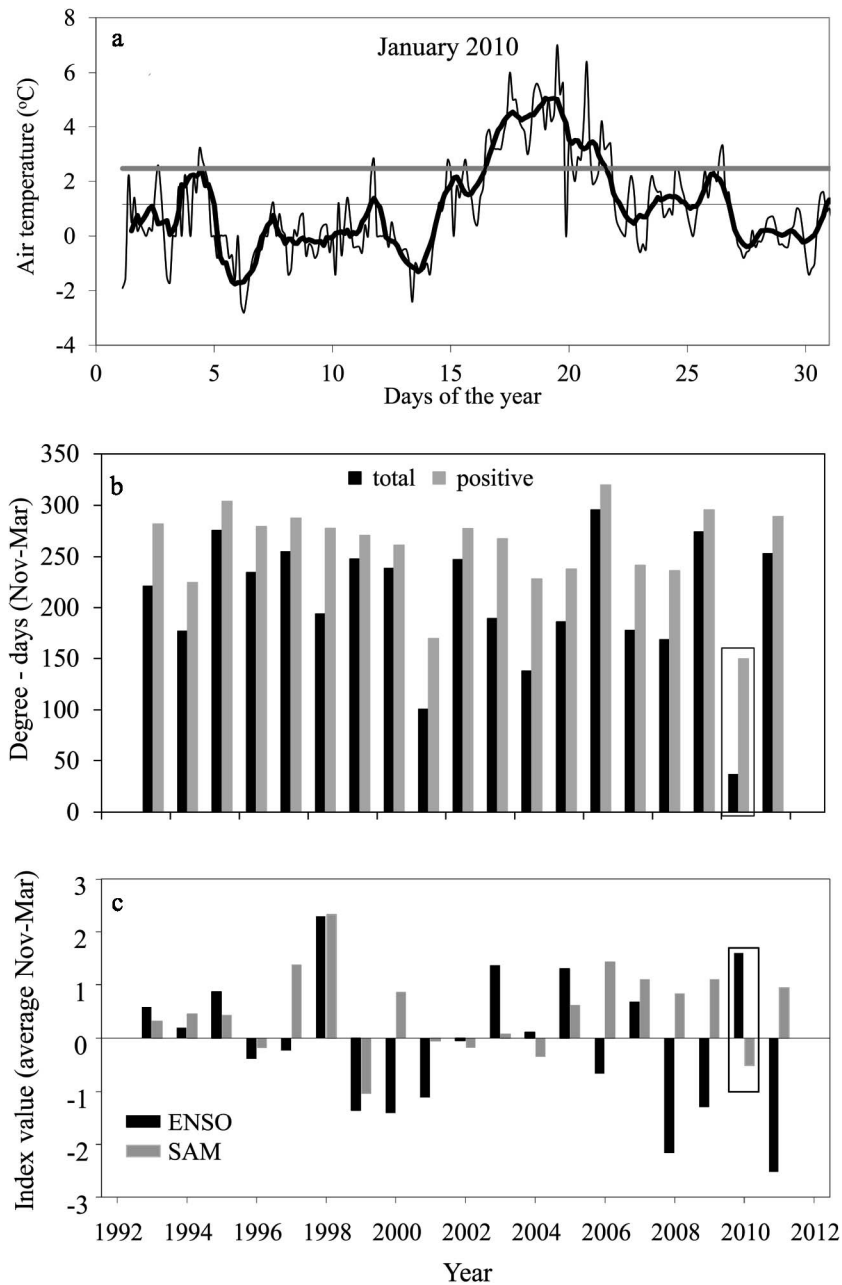


Fig. 2. Meteorological conditions during January 2010 in the South Shetland Islands. (a) Daily average air temperature (thin line) and 10 d moving average (thick line). The thick continuous line depicts the average 1991–2009 value at PC. The thin continuous line shows the average value for January 2010. (b) Total and positive degree-days (*see* Methods section) for the spring–summer period (November–March) from 1993 to 2011. (c) ENSO and SAM index values. The square highlights year 2010.

and December 2009 ( $-1.4^{\circ}\text{C}$  and  $-0.3^{\circ}\text{C}$ , respectively). Total and positive degree-days for the November–March period are plotted in Fig. 2b and show that austral summer 2010 was anomalously cold. Moreover, high and positive ENSO and negative SAM index values were observed during austral spring–summer 2009–2010 (Fig. 2c), a combination that has not been observed in the past 20 yr in the area (except in 2004, although with a lower ENSO index than in 2010).

A cubic relationship between ChlaMax and total degree-days was observed, as well as an almost cyclic relationship with ENSO, and a linear relationship with SAM. When fitting this information with ChlaMax by using the information-theoretic approach with data from the last 20 yr, it can be seen that model 1 is best supported by the data (Table 2) when only total degree-days are included in the equation. The relative probability of this model is 0.78. The second most probable of the chosen set also includes

Table 2. Models of maximum chlorophyll *a* (Chl*a*Max) fitted to environmental data. AICc, corrected Akaike Information Criterion;  $\Delta$ , differences between models. The probability of each model is indicated. Environmental variables: SA, SAM index; EN, ENSO Index; DD, total degree-days for the austral spring–summer season (November to March). The models are ranked according to their AICc; the lowest AICc corresponds to the one for which loss information is minimal.

Model formulation	AICc	$\Delta$	Probability
$\sqrt{\text{Chl}a\text{Max}} = \text{DD} + \text{DD}^2 + \text{DD}^3$	59.95	0.00	0.784
$\sqrt{\text{Chl}a\text{Max}} = \text{SA}$	60.09	3.15	0.136
$\sqrt{\text{Chl}a\text{Max}} = \cos(2\pi\text{EN}) + \sin(2\pi\text{EN})$	63.50	6.56	0.030
$\sqrt{\text{Chl}a\text{Max}} = \text{DD} + \text{DD}^2 + \text{DD}^3 + \text{SA}$	65.90	8.59	0.009
$\sqrt{\text{Chl}a\text{Max}} = \cos(2\pi\text{EN}) + \sin(2\pi\text{EN}) + \text{SA}$	66.14	9.19	0.008
$\sqrt{\text{Chl}a\text{Max}} = \text{DD} + \text{DD}^2 + \text{DD}^3 + \cos(2\pi\text{EN}) + \sin(2\pi\text{EN})$	67.69	10.74	0.004
$\sqrt{\text{Chl}a\text{Max}} = \text{DD} + \text{DD}^2 + \text{DD}^3 + \cos(2\pi\text{EN}) + \sin(2\pi\text{EN}) + \text{SA}$	68.34	11.39	0.003

the SAM index. Among the set of models we defined, total degree-days in first place and to a lesser extent total degree-days in combination with SAM index seem to be the best predictors of maximum seasonal Chl *a*.

Average wind speed in PC for January during the 1991–2009 period was significantly higher than in January 2010 ( $p < 0.05$ ; Fig. 3a). Anomaly for January 2010 wind speed (Schloss et al. 2012) was  $-1.5 \text{ m s}^{-1}$  and was also negative during November and December 2009 ( $-3.1$  and  $-0.1 \text{ m s}^{-1}$ , respectively). Wind speeds in January 2010 were slightly but significantly higher in PC than in AB ( $7.3 \pm 3.9$  and  $5.5 \pm$

$2.1 \text{ m s}^{-1}$ , respectively; Kolmogorov–Smirnov test,  $p < 0.05$ ). Notably, the dominant wind direction in both AB and PC is west–west northwest and usually follows the main axis of PC. In contrast, during January 2010, the average direction was east (Fig. 3b,c) in both PC and AB (only PC data depicted in the figure).

*Water column characteristics at PC and AB in January 2010*—Thermal and density stratifications were evident starting in early January and lasting to the end of the month (Fig. 4a,b) at both sites; positive temperatures were

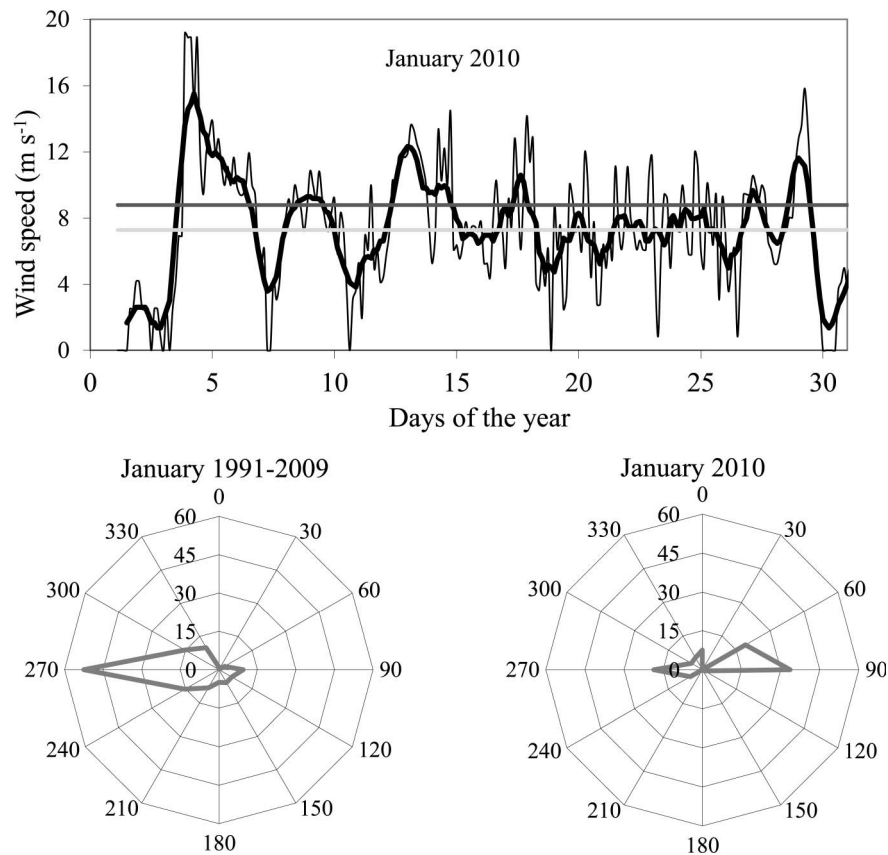


Fig. 3. (a) Wind speed during January 2010 in the South Shetland Islands. The dark straight line depicts the average 1991–2009 value at PC. The pale line shows the average value for January 2010. (b) Wind direction in PC during the January for the 1991–2009 period, and (c) during January 2010.

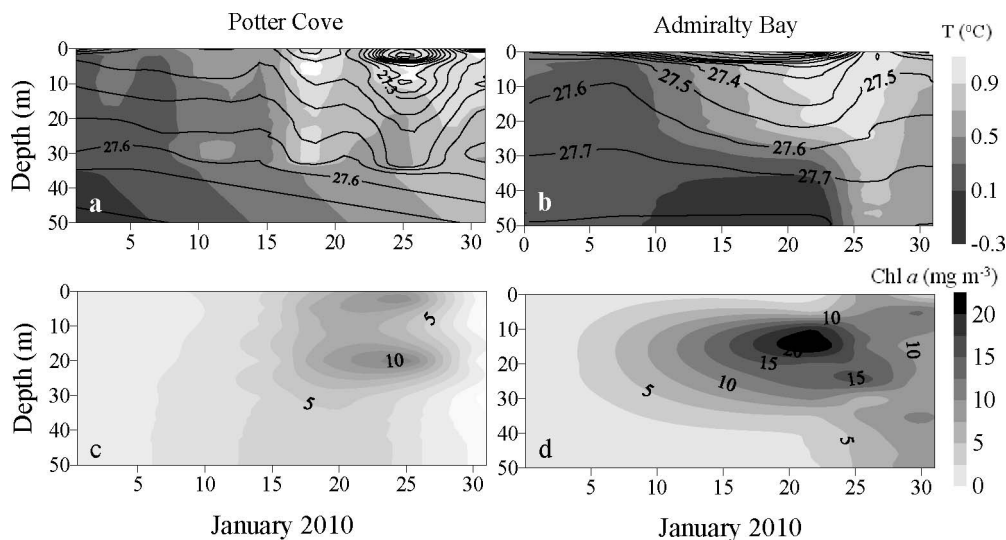


Fig. 4. Profiles from Potter Cove and Admiralty Bay of (a,b) seawater temperature, depicted as shaded areas, and the anomaly of the density, plotted on top as continuous isolines ( $\sigma_t$ ), and (c,d) chlorophyll *a*.

observed at the water surface (above 40 m water depth). A noteworthy feature was the strong density stratification, observed at both sites, but more markedly expressed in AB. Before this date, sea ice floes and growlers and bergy bits originating from disintegrating glacier frontal discharge were present at both sites, sometimes preventing sampling in the area. Nutrient data are not available for PC during the bloom period. In AB average nitrate and phosphate concentrations (Table 1) were not limiting during that period. Minimum nitrate and phosphate concentrations were 14.2 and 2.9  $\mu\text{mol L}^{-1}$ , respectively. After the bloom period,  $\text{NO}_3^-$  concentrations were again close to the maximal winter values  $> 30 \mu\text{mol L}^{-1}$ , indicating rapid nutrient replenishment after consumption. In PC, after the bloom period, nutrients attained high concentrations (Table 1). Here, minimum values were 24  $\mu\text{mol L}^{-1}$  and 2  $\mu\text{mol L}^{-1}$ , for  $\text{NO}_3^-$  and  $\text{PO}_4^{3-}$ , respectively. In January 2010 the average light attenuation coefficient,  $K_d$ , in PC was  $0.22 \pm 0.02$ , varying between 0.18 and 0.26, in relation to the TPM concentration in the water column (Table 1; maximum: 18  $\text{g m}^{-3}$ ). In AB, average  $K_d$  was  $0.06 \pm 0.04$  and varied only between 0.04 and 0.14 (data only available for the bloom period).

*Depth of turbulent mixing ( $Z_t$ ) vs. critical depth ( $Z_c$ )*—In AB, adequate physical conditions for phytoplankton growth were apparent since Sverdrup critical depth values  $Z_c$  exceeded the wind-induced turbulent vertical displacement of particles  $Z_t$  by  $> 15$  m during the entire month, thus allowing phytoplankton cells to remain in well-illuminated conditions (Fig. 5a). Although in PC the difference between these two depths was smaller than in AB, maximum  $Z_t$  was almost always shallower than  $Z_c$  (Fig. 5b). On only one occasion, around 12 January 2010, the maximal estimated  $Z_t$  reached  $Z_c$  for a short time, but remained shallower than  $Z_c$  by  $\sim 20$  m in the rest of the time. Photosynthetic particles were thus retained in well-illuminated surface waters for almost the whole study period. The difference between AB and PC

can be related to a lower  $K_d$  calculated for AB than for PC ( $0.20 \pm 0.03$  and  $0.23 \pm 0.02$ ; ANOVA  $p < 0.05$  for AB and PC, respectively).

In order to test the robustness of the approach and the validity of the interpolations performed in the modeling process, the same analysis was further applied to all the available data in both AB and PC areas since 1992. Given the amount of information required to perform the present analysis, for AB, it was only possible to add the analysis for the season of January 2007, whereas seasons corresponding to January of the years 1992, 1996, 1999, 2000, 2001, 2008, 2009, and 2011 were further analyzed for PC. Two seasons, apart from 2010, were chosen in this work as representatives of the different situations encountered in the analysis, namely January 2001 and January 2011 (both are only available in PC). No comparable bloom was observed during any of these seasons: maximum Chl *a* values ranged between 1.1 and 4.5  $\text{mg m}^{-3}$  (Fig. 6). The formalization of the model for 2001 showed that  $Z_c$  was on average deeper than  $Z_t$ . However, the longest duration of these favorable conditions was only 6 d, therefore not allowing significant phytoplankton accumulation. This was also the case in years 1996, 1999, 2000, 2008, and 2009 (Fig. 6). Interestingly, in the summer that followed our exceptional bloom year in 2010, i.e., in January 2011 (and also in 1992, as well as in AB in 2007),  $Z_c$  vs.  $Z_t$  conditions were found equally adequate for phytoplankton growth for 25 uninterrupted days, and although phytoplankton blooms developed, Chl *a* concentrations in PC never reached concentrations higher than 4  $\text{mg m}^{-3}$  (Fig. 6). Further, concentrations of inorganic macronutrients in 2011 were high enough not to limit phytoplankton growth (Table 1). Minimal values were 20 and 1.3  $\mu\text{mol L}^{-1}$  for  $\text{NO}_3^{2-}$  and  $\text{PO}_4^{3-}$ , respectively. Total suspended particulate matter concentrations were higher and more variable in 2011 than in 2010 (Table 1), with maximum concentrations of 23  $\text{g m}^{-3}$ .

The analysis of the stepwise multiple regression shows that the  $Z_c : Z_t$  ratio is significantly ( $p < 0.01$ ) correlated to

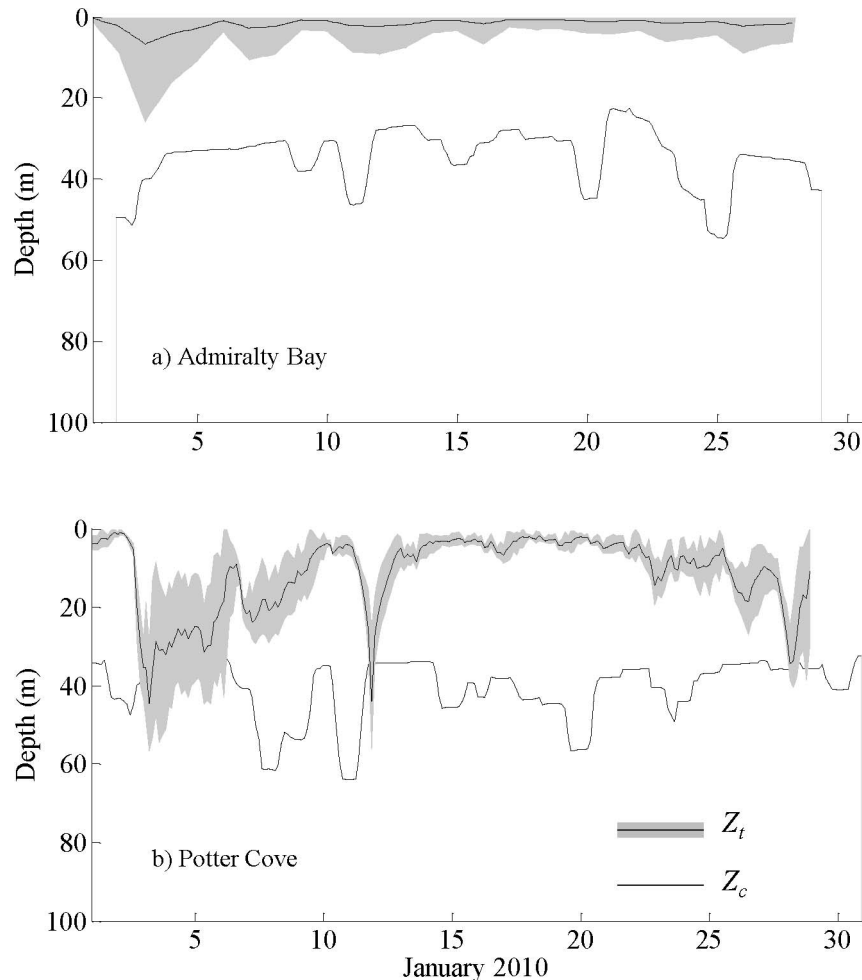


Fig. 5. Depth for the critical depth,  $Z_c$ , and turbulent mixing depth,  $Z_t$ , for (a) AB and (b) PC. Light shadowed area around  $Z_t$  represents the depth interval (minimum and maximum) estimated for cell's vertical excursions based on wind stress duration (minimum  $t = 3$  h; maximum  $t = 24$  h). No phytoplankton growth is expected below the dark line (i.e., depths  $> Z_c$ ). Both  $Z_c$  and  $Z_t$  are in meters.

Chl  $a$ , on its own explaining 75% of the variation in annual Chl  $a$  maxima. Air temperature (degree-days) was not significantly correlated when considering the 11 yr for which information on  $Z_c:Z_t$  was available ( $p = 0.12$ ); when considered together with the  $Z_c:Z_t$  ratio, the explained variance attains 82%. Duration was not significantly correlated to Chl  $a$  ( $p = 0.66$ ).

A (nonlinear) relation was found for maximum Chl  $a$  values and air temperature combining PC and AB data (model 1, Table 2). Considering only maximum summer values, the model including only air temperatures presents the lowest corrected AICc (Fig. 7), suggesting that the water column structure and light field are significantly and primarily influenced by air temperature. The second best model included also the SAM index, but models including ENSO presented much higher AICc.

*The phytoplankton bloom in January 2010*—Phytoplankton biomass, expressed as Chl  $a$  concentration, presented values  $< 3$  mg Chl  $a$   $m^{-3}$  at the beginning of the study

period. By 10 January 2010, an intense accumulation started, reaching high concentrations in both study areas (Fig. 4c,d). Although the information of the sampling points at each site was merged for the comparison of both places, it is worth mentioning that in AB, a maximal concentration of 23.5 mg Chl  $a$   $m^{-3}$  was observed at 15 m depth in the innermost station on 22 January 2010. At the outer stations, maxima were around 15.9 and 10.1 mg Chl  $a$   $m^{-3}$  on 02 January 2010 (no sampling was carried out in these two latter stations on 22 January 2010). Biomass concentrations were somewhat lower in PC than in AB, with maxima observed at 20 m on 18 January 2010 (14.7 mg Chl  $a$   $m^{-3}$ ) and 25 January 2010 (11.2 mg Chl  $a$   $m^{-3}$ ) for the inner and central sampling stations, respectively.

*Composition of phytoplankton assemblages*—The peak in phytoplankton biomass was due to blooms of large centric diatom in both areas. *Porosira glacialis* and *Thalassiosira antarctica* were the dominant species in PC, reaching densities up to  $1.8 \times 10^5$  cells  $L^{-1}$  and together accounting

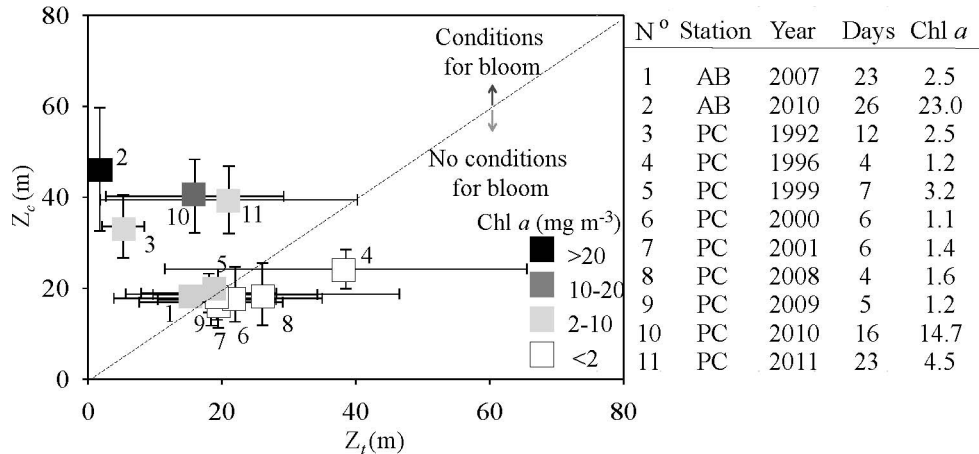


Fig. 6. Average conditions for blooms at AB and PC. The squares' centers correspond to the average  $Z_c: Z_t$  conditions during each season. Error bars around the squares indicate standard deviations of  $Z_c$  and  $Z_t$  for each season. The duration of  $Z_c > Z_t$  as well as the maximum Chl *a* for each season are indicated in the table at the right of the figure. The area below the line  $Z_c = Z_t$  depicts the conditions for which phytoplankton growth and accumulation is not possible.

for > 90% of total phytoplankton carbon biomass. The diatom bloom decayed after 1 week at the innermost station while it was still evident in the outer station, where it was notably enriched with the pennate diatom *Pseudogomphonema kamtschaticum*. After the study period in January 2010, diatoms were gradually replaced by smaller cryptophytes, which reached concentrations up to  $8.5 \times 10^5$  cells  $L^{-1}$  towards the end of February. In AB a high bloom of large diatoms (maximum  $3.8 \times 10^5$  cells  $L^{-1}$ ), such as *T. ritscheri* and *T. antarctica*, dominated the phytoplankton community. The bloom progressed from the bay's mouth at the end of December and beginning of January to sites located inside the bay. After the bloom had declined in

February, the phytoplankton community was dominated by prymnesiophytes and cryptophytes.

## Discussion

*Meteorological conditions during January 2010*—For the global ocean in general and for polar areas in particular, a declining trend in Chl *a* has been estimated for the last century (Boyce et al. 2010), which is related to a concurrent temperature increase. Our results show that warmer temperatures (higher degree-days) are associated with lower Chl *a* values. Similarly, the high 2010 bloom corresponded to an exceptionally cold year.

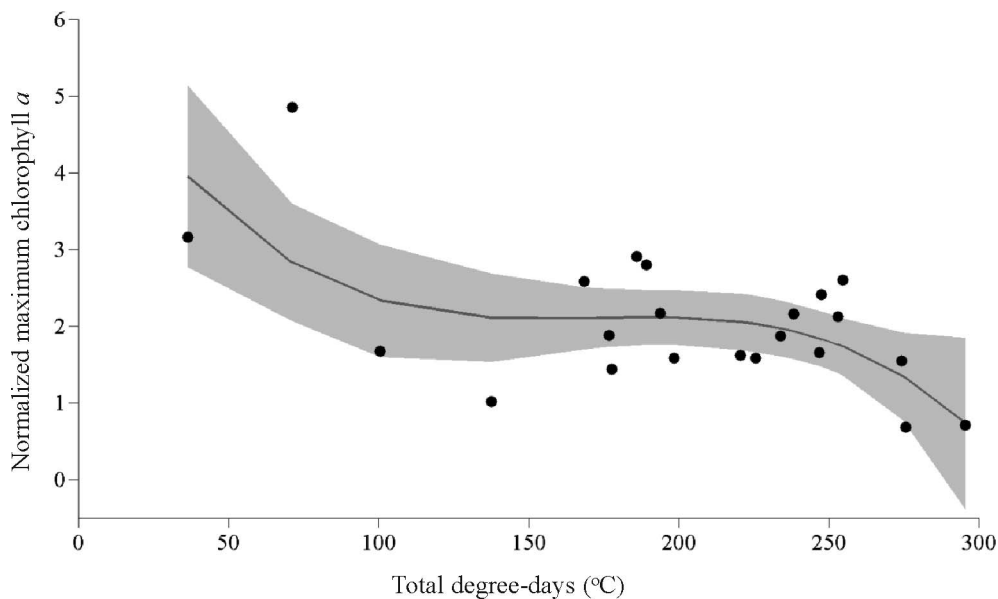


Fig. 7. Relation between spring-summer temperatures (total degree-days) and maximum Chl *a* values (after a square-root transformation of the values in  $mg\ m^{-3}$ ) for the period 1992–2011 in Potter Cove and Admiralty Bay, following the information-theoretic approach. The best fit was found for Eq. 1 (see Table 2). The shadowed area depicts the confidence interval.

According to Costa and Agosta (2012), an anomalous stationary cyclone to the northwest of the Antarctic Peninsula and an anticyclone over the Southeast Pacific Ocean persisted throughout the summer 2010. This can be related to positive sea surface temperature anomalies in the South Pacific, over the source region of the cyclone, through the generation of locally increased mean-flow baroclinicity. Costa and Agosta (2012) also describe an anomalous easterly wind component during this season, which could further favor cold temperature anomalies over the study area on a regional scale. Apart from their effect on air temperatures, during the usual high wind–intensity seasons, dominant easterly winds were shown to promote surface-water circulation out of PC, which is then replaced by nutrient-rich deeper waters (Schloss et al. 2002). However, the relatively weak wind speed observed especially at the beginning of the 2009–2010 spring–summer season enabled local stabilization of bloom conditions favoring a lower  $Z_t$  and a higher  $Z_c:Z_t$  ratio, further increasing the residence time of cells in the photic zone, and allowing for high phytoplankton accumulation in the cove.

In a previous study (Schloss et al. 2012), it has been shown that average Chl *a* concentrations are significantly (cross-) correlated with the SAM index, although the response varied with the depth and the location (station) considered. This is similar to the results found when analyzing the whole data set (i.e., including seasons other than just spring–summer; Schloss et al. 2012). Although the results of the multiple regression analysis between Chl *a* and temperature (as degree-days) for the data from the 11 yr for which the  $Z_c:Z_t$  ratio was available were not significant, when using data from 22 yr for which both temperature and Chl *a* data were available, the best model relating climatic indexes (ENSO, SAM, and air temperature, as degree-days) to maximum Chl *a* values was obtained for the cubic relation between air temperature only as the only independent variable. These results suggest that air temperature is a good summarizing factor to predict maximum Chl *a* concentrations. Moreover, the use of this second model contributes to explain the difference in maximum Chl *a* concentrations attained during these two summers, which can be related to the air temperature (253.01 total degree-days in 2011 in contrast with 36.48 total degree-days during 2010). This suggests that the Temperature–Chl *a* model could even have a predictive value for the determination of maximum Chl *a* concentrations that could be potentially attained. However, the fact that most of the data are in the middle zone of the curve, when total degree-days values are between 130°C and 230°C and lay outside the confidence interval, points toward other important factors influencing maximum Chl *a* values. This will be discussed in the next sections.

*Hydrology, nutrients, and the phytoplankton bloom*—During other summer seasons, under intense wind-mixing conditions, resuspended microbenthic diatoms, more than growing planktonic microalgae, were observed in the water column (Kopczyńska 2008). Nutrient (nitrate and phosphate) concentrations, as shown for both years 2010 and 2011 for both PC and AB, and as previously determined for

the study area (Schloss and Ferreyra 2002), were not limiting phytoplankton growth; micronutrients such as iron (Fe) have been shown to abound in particles generated by subglacial erosion and thus Fe appears nonlimiting in the PC area (Dick et al. 2007), as also generally observed in the region of the South Shetland Islands, which are sources of natural iron enrichment in the Antarctic Peninsula region (De Jong et al. 2012). Phytoplankton cells might therefore grow and accumulate when physical conditions are adequate for it, although this has not been previously observed to the extent found in the present work. Nutrient values in AB are generally nonlimiting for phytoplankton growth, both due to the inflow from the land (mainly from penguin rookeries) and due to water column instability, where turbulent mixing and advection cause the continuous replenishment of nutrients in the euphotic zone (Nędzarek and Rakusa-Suszczewski 2004).

The relation between the critical depth ( $Z_c$ ) and the turbulent mixing depth ( $Z_t$ ) has explained phytoplankton dynamics in the PC area for the last 20 yr (Schloss et al. 2012). During this period, average summer values were normally below 1 mg Chl *a* m<sup>-3</sup>, although occasional blooms of ~ 4 mg Chl *a* m<sup>-3</sup> were also found. In the present work the conceptual, threshold-based model of Schloss et al. (2002) is refined to determine a set of criteria favoring accumulation in a time-evolving manner, using available in situ data. This detailed analysis of the 2010 data set shows that for both areas (AB and PC) adequate light and mixing conditions prevailed that allowed a phytoplankton bloom to develop. In AB  $Z_c$  was deeper than in PC, allowing for light penetration in the water column during January 2010 to values similar to those previously reported (average 1% of surface irradiance around 35 m; Rakusa-Suszczewski 1995). Although no information on particle concentrations is available for AB, the relatively cold 2010 summer very likely caused the late onset of glacier melting observed in the area (C. Dominguez and A. Eraso unpubl.; <http://doi.pangaea.de/10.1594/PANGAEA.744785>) and prevented intensive particle-loaded glacial meltwater runoff into the coastal areas. The number of positive degree-days (Fig. 2b) is a widely used indicator of the amount of glacier melting despite the complex glacier energy-balance processes involved (Braithwaite 1995). This variable was significantly lower in 2010 compared to the 20 yr average, contributing to explain that glacier runoff was lower than during average years. Since particulate matter in the water column mainly comes from glacier runoffs, colder temperatures during summer 2010 explain their observed low concentrations in PC. In addition, in January 2010 surface warming in AB because of unusually slow wind speeds led to a very shallow mixed layer and a pycnocline that was sharper than the usual uniform vertical profiles (Catewicz and Kowalik 1983), therefore increasing water column stability. In most other years, strong mixing prevented the formation of a strong, spring–summer thermo-halocline, as would be expected in a closed basin (Catewicz and Kowalik 1983).

In PC  $K_d$  values for light attenuation were higher than in AB, but still considerably lower than those reported from previous years (Schloss and Ferreyra 2002). This is in clear

relation with lower than usual particulate matter concentrations. In consequence, Chl *a* concentrations in AB were higher than in PC. The different methods used to estimate pigment concentrations in both places does not explain these differences, since both methods are calibrated with commercial chlorophyll standards, and spectrophotometric and HPLC analyses give comparable results when concentrations of degradation products are low (Jodłowska and Latała 2011). Moreover, similar phytoplankton assemblages of large centric diatoms were dominant in both areas.

*Applying the physical–biological model to other years—*Applying the same analysis to the 11 austral seasons (Fig. 6), the regression among Chl *a* and the  $Z_c:Z_t$  ratio as well as its duration and air temperature, a high fraction of the variance (75%) was explained by the  $Z_c:Z_t$  ratio, therefore confirming its validity in turbulent coastal waters where mixing dominates the water column and light penetration is strongly influenced by terrigenous particles. In other years we analyzed for comparison (i.e., years 1999, 2000, 2001, 2008 and 2009), favorable light penetration and mixing conditions never lasted > 6 consecutive days, which we considered not long enough to allow phytoplankton accumulations of even  $3 \text{ mg m}^{-3}$  Chl *a* (Schloss et al. 2002). In 2011  $Z_c > Z_t$  rates were favorable for at least 25 consecutive days but phytoplankton biomass did not exceed  $4 \text{ mg Chl } a \text{ m}^{-3}$ , which corresponds to a less massive bloom than in 2010. This, as well as the results of the multiple correlation, which showed no significant correlation between maximum Chl *a* concentrations and the duration of the adequate  $Z_c:Z_t$  conditions, indicate that duration might not be related to the intensity of phytoplankton blooms. To attain concentrations as high as those observed in 2010 (i.e., >  $10 \text{ mg m}^{-3}$  Chl *a*), phytoplankton cells must necessarily spend a minimum time in a light- and nutrient-rich environment, but other conditions must be present, some of which remain to be investigated and are discussed below.

The wind direction might be an important factor driving the level of horizontal accumulation through advection in semi-enclosed bays like PC and AB. The obvious difference in the dominant direction between January 2010 and January for the 1991–2009 period has probably an effect on this. Temperatures were higher in 2011 than in 2010 (Table 1). Higher temperatures can increase phytoplankton growth rates and photosynthesis (Neori and Holm-Hansen 1982; Thomas et al. 2012). However, total particle concentrations were also higher in PC in January 2011 than in 2010 (Table 1), probably related to the earlier onset of glacier melting, which started already in December 2010 with volumes 30 times those of December 2009 (C. Dominguez and A. Eraso unpubl.), therefore affecting  $Z_c$  that depends on the attenuation coefficient  $K_d$ , and contributing to explain the lower  $Z_c:Z_t$  ratios observed during that season (Fig. 6).

Another factor limiting phytoplankton growth in years with early onset of melting is lowered salinity from meltwater input. In 2010 surface salinity values were higher than those reported as typical for the area, between 33.41–33.76 (Rakusa-Suszczewski 1995). However, in 2011, due to

early onset of glacier melting (C. Dominguez and A. Eraso unpubl.), average sea surface salinity in PC was significantly lower than in 2010 (Table 1; ANOVA,  $p < 0.01$ ); salinities < 33 were indeed measured during the 2011 season in waters below 5 m. Experimental work has shown that low salinity is a stress source for plankton organisms (Petrou et al. 2011). When the phytoplankton community from PC was grown under contrasting salinity conditions (30 vs. 34), a significantly lower biomass accumulation was observed after 24 h exposure to low salinity ( $3.4 \pm 1.9 \text{ mg Chl } a \text{ m}^{-3}$ ) than under normal salinity conditions ( $9.4 \pm 1.1 \text{ mg Chl } a \text{ m}^{-3}$ ,  $p < 0.05$ ). After 4 d of exposure, a significant inhibition of the instantaneous growth rate ( $-0.5 \pm 0.18$  vs.  $1.5 \pm 0.22 \text{ d}^{-1}$ , for low and normal salinity, respectively;  $p < 0.05$ ) and an increase in concentrations of TBARS (2-thiobarbituric acid reactive substances), which indicate membrane damage by the way of lipid peroxidation, were observed ( $4.09 \pm 1.56$  vs.  $0.85 \pm 0.05 \text{ pmol cell}^{-1}$ , for low and normal salinity, respectively;  $p < 0.05$ ). Moreover, at that time, contrasting phytoplankton assemblages started to develop in both treatments, with centric diatoms such as *Odontella weissflogii* and *Chaetoceros* spp. continuing to grow under normal salinity, but being replaced by small pennate diatoms under low-salinity conditions (M. P. Hernando et al. unpubl.). Persistent favorable  $Z_c:Z_t$  ratios therefore constitute a necessary requirement for bloom formation, but are not sufficient to support high productivity.

*Composition of phytoplankton assemblages—*Phytoplankton assemblage composition during January 2010 in AB and PC do not differ qualitatively from what has been observed in other seasons in the area or in other Antarctic areas. The contribution of pelagic micro-sized diatoms in phytoplankton blooms during the growing season has been previously observed in KGI, both in the Maxwell Bay–PC area (Ahn et al. 1997; Schloss et al. 1997) and in AB (Kopczyńska 1981). The dominant species found during the 2010 bloom (i.e., *Porosira glacialis*, *Thalassiosira antarctica*, and *T. ritscheri*) are usual components of Antarctic phytoplankton. For example, *T. antarctica* is the year-round dominant diatom in AB (Kopczyńska 1996) and has also been observed to produce large biomass accumulations in the Bellingshausen and Weddell Seas (Edwards et al. 1998; Smetacek et al. 1992). On the other hand, and according to paleoecological information, *T. antarctica* and *Porosira glacialis* are typical summer bloom species in Antarctica with similar ecological preferences, usually found in cold coastal waters at the sea ice edge (Pike et al. 2009). Moreover, the same authors highlighted the fact that high fluxes of *T. antarctica* and *P. glacialis* resting spores to the sediment are associated with high concentrations of winter and spring sea ice that promote the buildup of large vegetative cell populations. This could have added to their massive presence in January 2010. The third bloom-forming diatom species found during our study, *T. ritscheri*, has been described as an important component of phytoplankton communities in AB (Lange et al. 2007). Altogether, this highlights the fact that the phytoplankton assemblage composition encountered during the massive bloom event was not exceptional during 2010, contrary to the abundance of the cells.

*Other factors affecting phytoplankton accumulation*—So far here we have only considered “bottom-up” processes. Macrozooplankton are typically abundant after a peak of phytoplankton, as suggested by Kopczyńska (1981) in AB and the Antarctic Peninsula, where grazing of phytoplankton by euphausiids (such as krill, *Euphausia superba* and *E. crystallorophias*) and different species of copepods grazing are responsible for the breakdown of microalgae biomass at that moment. On the other hand, grazing by microzooplankton has been suggested to control Antarctic phytoplankton accumulation in coastal areas during spring–summer (Brandini 1993). Microzooplankton has frequently been neglected as a controlling factor of phytoplankton biomass. In a modeling effort, Walsh et al. (2001) assumed that diatoms are consumed by krill, salps, and copepods. They further suggested that only small cells such as *Phaeocystis antarctica* in their single-cell motile stage and cryptomonads are preyed upon by protozoans. While this may be adequate for eutrophic oceans and for areas where blooms usually occur such as the western Antarctic Peninsula area (Smith et al. 2008), the model may underestimate the effect of grazing by microzooplankton in environments like KGI. Sherr and Sherr (2007) showed that microzooplankton (heterotrophic dinoflagellates and ciliates) can actively prey on nanophytoplankton and microphytoplankton size cells and even ingest chain-forming diatoms in the same size range. Hence, here we hypothesize that heterotrophic dinoflagellates, which represent a large part of Antarctic microzooplankton biomass, can be responsible for significant losses of daily primary production. The results of Price and Steinberg (2013) suggest that microzooplankton may usually control the start of blooms in areas like coastal KGI, when Chl *a* values are low (i.e.,  $< 0.5 \text{ mg m}^{-3}$ ; Sherr and Sherr 2009) and substantially contribute to their decay (Calbet and Landry 2004). However, phytoplankton blooms are normal features in many other coastal Antarctic areas, and this can be attributed to the generally low growth rates of heterotrophic protists in cold waters, compared with phytoplankton (Rose and Caron 2007), resulting in uncoupled grazing activity of microzooplankton regarding phytoplankton growth rates. We speculate that anomalously cold conditions, such as those observed in 2010, may have reduced microzooplankton grazing pressure and allow phytoplankton biomass accumulation. A physiological explanation to support this hypothesis is that microzooplankton (as well as copepods) have a stronger growth response to temperature than phytoplankton, with lower temperatures reducing growth and then grazing pressure by these herbivores (Rose and Caron 2007; Chen et al. 2012). Following the same line of analysis, Aberle et al. (2012) experimentally showed that higher temperatures reduced the mismatch between the abundance peaks of phytoplankton and both copepods and protozoan biomass maxima for Baltic Sea plankton, therefore strengthening “top-down” control of phytoplankton. The observed bloom during the particularly cold summer of 2010 thus supports the hypothesis of Irigoien (2005) that phytoplankton blooming species are those able to escape control by microzooplankton. Temperatures in 2010 would have been around the

optimum for growth of grazers such as krill (Atkinson et al. 2006), but their abundance was low during January 2010 (M. S. Hoffmeyer et al. unpubl.). The lack of a massive bloom in January 2011 can presumably be attributed to higher grazing pressure than in January 2010, in addition to possible effects of low-salinity stress on cells in 2011.

Rapid removal of cells from the water column by sedimentation can be invoked as another possible reason for low Chl *a* concentrations. Indeed, very high sedimentation rates have been measured for PC phytoplankton (Schloss et al. 1999), although the proportion of living phytoplankton was relatively low, consistent with the low phytoplankton biomass observed during that study.

*Synthesis of the results from the two models*—In a study based on a 19 yr time series in PC, Schloss et al. (2012) found that air temperature presented significant positive correlations with surface-water temperature and negative correlations with salinity. In turn, these factors also correlated with concentrations of TPM, therefore contributing to explain the indirect effects of the input of particles from glacier melting on phytoplankton growth via light penetration (Schloss and Ferreyra 2002). In this sense, air temperature plays a key role in the dynamics of this coastal ecosystem. Results from an information-theoretic model approach, combined with the physical–biological model proposed by Schloss et al. (2002) and further improved here, are consistent with this hypothesis. The information-theoretic model, which relates the maximum observed concentration of Chl *a* (Chl*a*Max) to surface air temperature, expressed in terms of total degree-days, shows three main tendencies (Fig. 7). At highest temperatures there is a marked decreasing trend of Chl *a* as temperature increases (between  $\sim 250$  and  $300$  total degree-days); at intermediate temperatures  $\sim 100$  and  $250$  total degree-days, the model displays a plateau with a smooth decline at lower temperatures; and finally, a sharp increase in Chl*a*Max can be observed at lower temperatures (below  $\sim 100$  total degree-days, which includes 2010 results). Our interpretation is that the trend at higher temperatures is related with the light: mixing control of Chl *a* through light limitation, as proposed in our previous papers (Schloss et al. 2002, 2012). The plateau is explained by a steady equilibrium between physical processes (bottom-up) and grazing (top-down) processes. The variation in the relative weight of these factors probably contributes to explain the points outside the confidence interval. Finally, the low temperature trend may be associated with the physical control of phytoplankton (long duration of appropriate  $Z_c$  and  $Z_r$  conditions, see Fig. 6), but in this case with a simultaneous relaxation of the top-down control, as discussed in the previous section. The interaction between these factors favored the significant biomass accumulation in 2010. This interpretation is consistent with the theory of regime shifts, which are defined as prominent changes from a relatively stable state to another (Scheffer et al. 2001). In our statistical model, the plateau portion of the function denotes a stable condition, and both extremes of the function represent shifts. The modulation of these shifts is given by threshold values in temperature expressed as degree-days, which were followed by opposite direction trends. It should be noted that, with the available data set, we failed to detect

potentially new stable conditions. However, the threshold values of the two regime shifts suggest the existence of strong biological responses triggered by relatively small variations in the physical forcings. Given that phytoplankton is at the base of the Antarctic trophic food web, variations in physical parameters, such as temperature, may have significant consequences for the rest of the ecosystem.

In conclusion, the combination of a regional change in wind direction that favored the persistence of anomalously cold conditions and the favorable  $Z_c : Z_t$  ratios can be part of the explanation of the exceptional phytoplankton bloom in 2010. The generality of these results will depend on the frequency this combination of events will be observed in the future. The continuity of the long-term phytoplankton studies is therefore necessary to understand its future dynamics along the WAP. The  $Z_c : Z_t$  ratio proved to be a tool to adequately constrain the conditions for phytoplankton growth, although the inclusion of the biomass accumulation effect due to local wind direction, the duration of such conditions, and the absolute values for other variables (i.e., salinity) seem to be necessary to generalize the application of the model to the 2010 and 2011 seasons to represent the bottom-up processes controlling phytoplankton development. If top-down processes are also to be considered, mechanistic biological–physical coupled numerical models of marine planktonic systems may be the next logical step to pursue in further research studies.

#### Acknowledgments

We are very thankful to the personnel on both Carlini and Arctowski Stations for their great support in the field. Special thanks to Oscar González, Alejandro Ulrich, and Silvia Rodríguez for their overall help. The Argentinean National Meteorological Service (SMN) kindly provided meteorological information. In addition, we sincerely acknowledge Doris Abele from the Alfred-Wegener Institute for Polar and Marine Research for discussions in the field and for her long-lasting support with the instruments used for these analyses, and Philippe Archambault for statistical advice. Thanks also to Serge Demers, who supported part of this study. Finally, thanks to John Turner (British Antarctic Survey) for some thoughts about January 2010's meteorology. This study was supported by PICTO (Proyectos de Investigación Científica y Tecnológica Orientados) 35562 and PICT (Proyectos de Investigación Científica y Tecnológica) 2011 1320 to I.R.S. and is part of the Impact of climate induced glacial melting on marine coastal systems in the Western Antarctic Peninsula Region (IMCOAST, European Partnership in Polar Climate Science) supported by the European Polar Consortium–European Research Area–Net. Additional funding (Germany): Bundesministerium für Bildung und Forschung 03F0617A (A.V.B.) and 03F0617C (D.M.). Finally, we want also to sincerely thank two anonymous reviewers for their constructive comments with respect to our manuscript. Amending the manuscript in accordance with their suggestions has—in our eyes—definitely improved our work.

#### References

- ABERLE, N., B. BAUER, A. LEWANDOWSKA, U. GAEDKE, AND U. SOMMER. 2012. Warming induces shifts in microzooplankton phenology and reduces time-lags between phytoplankton and protozoan production. *Mar. Biol.* **159**: 2441–2453, doi:10.1007/s00227-012-1947-0
- AHN, I.-Y., H. CHUNG, J.-S. KANG, AND S.-H. KANG. 1997. Diatom composition and biomass variability in nearshore waters of Maxwell Bay, Antarctica, during the 1992/1993 austral summer. *Polar Biol.* **17**: 123–130, doi:10.1007/s003000050114
- ALMANDOZ, G. O., M. P. HERNANDO, G. A. FERREYRA, I. R. SCHLOSS, AND M. E. FERRARIO. 2011. Seasonal phytoplankton dynamics in extreme southern South America (Beagle Channel, Argentina). *J. Sea Res.* **66**: 47–57, doi:10.1016/j.seares.2011.03.005
- ATKINSON, A., AND OTHERS. 2006. Natural growth rates in Antarctic krill (*Euphausia superba*): II. Predictive models based on food, temperature, body length, sex, and maturity stage. *Limnol. Oceanogr.* **51**: 973–987, doi:10.4319/lo.2006.51.2.0973
- BOYCE, D. G., M. R. LEWIS, AND B. WORM. 2010. Global phytoplankton decline over the past century. *Nature* **466**: 591–596, doi:10.1038/nature09268
- BRAITHWAITE, R. J. 1995. Positive degree-day factors for ablation on the Greenland ice sheet studied by energy-balance modelling. *J. Glaciol.* **41**: 153–160.
- BRANDINI, F. P. 1993. Phytoplankton biomass in an Antarctic coastal environment during stable water conditions—implications for the iron limitation theory. *Mar. Ecol. Prog. Ser.* **93**: 267–275, doi:10.3354/meps093267
- BURNHAM, K., AND D. ANDERSON. 2002. Model selection and multi-model inference: A practical information-theoretic approach, 2nd ed. Springer.
- , ———, AND K. HUYVAERT. 2011. AIC model selection and multimodel inference in behavioral ecology: Some background, observations, and comparisons. *Behav. Ecol. Sociobiol.* **25**: 23–25, doi:10.1007/s00265-010-1029-6
- CALBET, A., AND M. R. LANDRY. 2004. Phytoplankton growth, microzooplankton grazing, and carbon cycling in marine systems. *Limnol. Oceanogr.* **49**: 51–57, doi:10.4319/lo.2004.49.1.0051
- CATEWICZ, Z., AND Z. KOWALIK. 1983. Harmonic analysis of tides in Admiralty Bay. *Oceanologia* **15**: 97–109.
- CHEN, B., M. R. LANDRY, B. HUANG, AND H. LIU. 2012. Does warming enhance the effect of microzooplankton grazing on marine phytoplankton in the ocean? *Limnol. Oceanogr.* **57**: 519–526, doi:10.4319/lo.2012.57.2.0519
- CLARKE, A., E. J. MURPHY, M. P. MEREDITH, J. C. KING, L. S. PECK, D. K. A. BARNES, AND R. C. SMITH. 2007. Climate change and the marine ecosystem of the western Antarctic Peninsula. *Philos. Trans. R. Soc. B* **362**: 149–166, doi:10.1098/rstb.2006.1958
- COSTA, A., AND E. AGOSTA. 2012. South Pacific quasi-stationary waves and anomalously cold summers in northernmost Antarctic Peninsula. *Geoacta* **37**: 73–82.
- DE JONG, J., V. SCHOEMANN, AND D. LANNUZEL. 2012. Natural iron fertilization of the Atlantic sector of the Southern Ocean by continental shelf sources of the Antarctic Peninsula. *J. Geophys. Res.* **117**: G01029, doi:10.1029/2011JG001679
- DENMAN, K., AND A. GARGETT. 1983. Time and space scales of vertical mixing and advection of phytoplankton in the upper ocean. *Limnol. Oceanogr.* **28**: 801–815, doi:10.4319/lo.1983.28.5.0801
- DICK, D., E. PHILIPP, M. KRIEWS, AND D. ABELE. 2007. Is the umbo matrix of bivalve shells (*Laternula elliptica*) a climate archive? *Aquat. Toxicol.* **84**: 450–456, doi:10.1016/j.aquatox.2007.07.005
- EDWARDS, E. S., P. H. BURKILL, AND M. A. SLEIGH. 1998. Microbial community structure in the marginal ice zone of the Bellingshausen Sea. *J. Mar. Syst.* **17**: 87–96, doi:10.1016/S0924-7963(98)00031-1

- GRASSHOFF, K., K. KREMLING, AND M. EHRHARDT. 1999. Methods of seawater analysis. Wiley-VCH.
- HERNANDO, M. P., AND G. A. FERREYRA. 2005. The effects of UV radiation on photosynthesis in an Antarctic diatom (*Thalassiosira* sp.): Does vertical mixing matter? *J. Exp. Mar. Biol. Ecol.* **325**: 35–45, doi:10.1016/j.jembe.2005.04.021
- HEWES, C. D., C. S. REISS, AND O. HOLM-HANSEN. 2009. A quantitative analysis of sources for summertime phytoplankton variability over 18 years in the South Shetland Islands (Antarctica) region. *Deep-Sea Res. I* **56**: 1230–1241, doi:10.1016/j.dsr.2009.01.010
- HOLM-HANSEN, O., B. G. MITCHELL, C. D. HEWES, AND D. M. KARL. 1989. Phytoplankton blooms in the vicinity of Palmer Station, Antarctica. *Polar Biol.* **10**: 49–57.
- IRIGOIEN, X. 2005. Phytoplankton blooms: A “loophole” in microzooplankton grazing impact? *J. Plankton Res.* **27**: 313–321, doi:10.1093/plankt/fbi011
- JEFFREY, S. W., R. F. C. MANTOURA, AND S. W. WRIGHT. 1997. Phytoplankton pigments in oceanography: Guidelines to modern oceanography. UNESCO Publishing.
- JODŁOWSKA, S., AND A. LATAŁA. 2011. The comparison of spectrophotometric method and high-performance liquid chromatography in photosynthetic pigments analysis. *Online J. Biol. Sci.* **11**: 63–69, doi:10.3844/ojbsci.2011.63.69
- KOPCZYŃSKA, E. E. 1981. Periodicity and composition of summer phytoplankton in Ezcura Inlet, Admiralty Bay, King George Island, South Shetland Islands. *Pol. Polar Res.* **2**: 55–70.
- . 1996. Annual study of phytoplankton in Admiralty Bay, King George Island, Antarctica. *Pol. Polar Res.* **17**: 151–164.
- . 2008. Phytoplankton variability in Admiralty Bay, King George Island, South Shetland Islands: Six years of monitoring. *Pol. Polar Res.* **29**: 117–139.
- KRAUS, S., M. MCWILLIAMS, AND Z. PECSKAY. 2007. New <sup>40</sup>Ar/<sup>39</sup>Ar and K/Ar ages of dikes in the South Shetland Islands (Antarctic Peninsula). In A. K. Cooper and C. R. Raymond [eds.], *Antarctica: A keystone in a changing world—Online Proceedings of the 10th ISAES*. Open-File Report 2007-1047, Short Research Paper 035. U.S. Geological Survey, doi:10.3133/of2007-1047.srp035
- LANGE, P. K., D. R. TENENBAUM, E. SANTIS BRAGA, AND L. S. CAMPOS. 2007. Microphytoplankton assemblages in shallow waters at Admiralty Bay (King George Island, Antarctica) during the summer 2002–2003. *Polar Biol.* **30**: 1483–1492, doi:10.1007/s00300-007-0309-8
- LASKOV, C., C. HERZOG, J. LEWANDOWSKI, AND M. HUPFER. 2007. Miniaturized photometrical methods for the rapid analysis of phosphate, ammonium, ferrous iron, and sulfate in pore water of freshwater sediments. *Limnol. Oceanogr.: Methods* **5**: 63–71, doi:10.4319/lom.2007.5.63
- MANTOURA, R. F. C., AND D. J. REPETA. 1997. Calibration method for HPLC, p. 407–428. In S. W. Jeffrey, R. F. C. Mantoura, and S. W. Wright [eds.], *Phytoplankton pigments in oceanography: Guidelines to modern methods*. UNESCO.
- MARSHALL, G. J. 2003. Trends in the Southern Annular Mode from observations and reanalyses. *J. Clim.* **16**: 4134–4143, doi:10.1175/1520-0442(2003)016<4134:TITSAM>2.0.CO;2
- MEREDITH, M. P., E. MURPHY, E. HAWKER, J. KING, AND M. WALLACE. 2008. On the interannual variability of ocean temperatures around South Georgia, Southern Ocean: Forcing by El Niño/Southern Oscillation and the Southern Annular Mode. *Deep-Sea Res. II* **55**: 2007–2022, doi:10.1016/j.dsr2.2008.05.020
- MIRANDA, K. M., M. G. ESPEY, AND D. A. WINK. 2001. A rapid, simple spectrophotometric method for simultaneous detection of nitrate and nitrite. *Nitric Oxide Biol. Chem.* **5**: 62–71, doi:10.1006/niox.2000.0319
- MONTES-HUGO, M., S. C. DONEY, H. W. DUCKLOW, W. R. FRASER, D. MARTINSON, S. E. STAMMERJOHN, AND O. SCHOFIELD. 2009. Recent changes in phytoplankton communities associated with rapid regional climate change along the western Antarctic Peninsula. *Science* **323**: 1471–1473.
- NĘDZAREK, A., AND S. RAKUSA-SUSZCZEWSKI. 2004. Decomposition of macroalgae and the release of nutrient in Admiralty Bay, King George Island, Antarctica. *Polar Biosci.* **17**: 26–35.
- NELSON, D. M., AND W. O. J. SMITH. 1991. Sverdrup revisited: Critical depths, maximum chlorophyll levels, and the control of Southern Ocean productivity by the irradiance-mixing regime. *Limnol. Oceanogr.* **36**: 1650–1661, doi:10.4319/lo.1991.36.8.1650
- NEORI, A., AND O. HOLM-HANSEN. 1982. Effect of temperature on rate of photosynthesis in Antarctic phytoplankton. *Polar Biol.* **1**: 33–38, doi:10.1007/BF00568752
- PETROU, K., M. A. DOBLIN, AND P. J. RALPH. 2011. Heterogeneity in the photoprotective capacity of three Antarctic diatoms during short-term changes in salinity and temperature. *Mar. Biol.* **158**: 1029–1041, doi:10.1007/s00227-011-1628-4
- PIKE, J., X. CROSTA, E. J. MADDISON, C. E. STICKLEY, D. DENIS, L. BARBARA, AND H. RENNSSEN. 2009. Observations on the relationship between the Antarctic coastal diatoms *Thalassiosira antarctica* Comber and *Porosira glacialis* (Grunow) Jørgensen and sea ice concentrations during the Late Quaternary. *Mar. Micropaleontol.* **73**: 14–25, doi:10.1016/j.marmicro.2009.06.005
- PIQUET, A. M. T., H. BOLHUIS, M. P. MEREDITH, AND A. G. J. BUMA. 2011. Shifts in coastal Antarctic marine microbial communities during and after melt water related surface stratification. *FEMS Microb. Ecol.* **76**: 413–427, doi:10.1111/j.1574-6941.2011.01062.x
- PRICE, L. M., AND D. K. STEINBERG. 2013. Microzooplankton community composition along the Western Antarctic Peninsula. *Deep-Sea Res. I* **77**: 36–49, doi:10.1016/j.dsr.2013.03.001
- PRUSZAK, Z. 1980. Currents circulation in Admiralty Bay (region of Arctowski station on King George Island). *Pol. Polar Res.* **1**: 55–74.
- RAKUSA-SUSZCZEWSKI, S. 1995. The hydrography of Admiralty Bay and its inlets, coves and lagoons (King George Island, Antarctica). *Pol. Polar Res.* **16**: 61–70.
- ROSE, J. M., AND D. A. CARON. 2007. Does low temperature constrain the growth rates of heterotrophic protists? Evidence and implications for algal blooms in cold waters. *Limnol. Oceanogr.* **52**: 886–895, doi:10.4319/lo.2007.52.2.0886
- SCHAEFFER, M., S. CARPENTER, J. A. FOLEY, C. FOLKE, AND B. WALKER. 2001. Catastrophic shifts in ecosystems. *Nature* **413**: 591–596, doi:10.1038/35098000
- SCHLOSS, I. R., D. ABELE, S. MOREAU, S. DEMERS, A. V. BERS, O. GONZÁLEZ, AND G. A. FERREYRA. 2012. Response of phytoplankton dynamics to 19-year (1991–2009) climate trends in Potter Cove (Antarctica). *J. Mar. Syst.* **92**: 53–66, doi:10.1016/j.jmarsys.2011.10.006
- , AND G. A. FERREYRA. 2002. Primary production, light and vertical mixing in Potter Cove, a shallow bay in the maritime Antarctic. *Polar Biol.* **25**: 41–48, doi:10.1007/s003000100309
- , ———, G. MERCURI, AND J. KOWALKE. 1999. Particle flux in an Antarctic shallow coastal environment: A sediment trap study. *Sci. Mar.* **63**: 99–111, doi:10.3989/scimar.1999.63s199
- , ———, AND D. RUIZ PINO. 2002. Phytoplankton biomass in Antarctic shelf zones: A conceptual model based on Potter Cove, King George Island. *J. Mar. Syst.* **36**: 129–143, doi:10.1016/S0924-7963(02)00183-5
- , H. KLÖSER, G. A. FERREYRA, A. CURTOSI, G. MERCURI, AND E. PINOLA. 1997. Factors governing phytoplankton and particulate matter variation in Potter Cove, King George

- island, Antarctica, p. 135–141. In B. Battaglia, J. Valencia, and D. W. H. Walton [eds.], Antarctic communities. Cambridge Univ. Press.
- SHERR, E., AND B. SHERR. 2007. Heterotrophic dinoflagellates: A significant component of microzooplankton biomass and major grazers of diatoms in the sea. *Mar. Ecol. Prog. Ser.* **352**: 187–197, doi:10.3354/meps07161
- , AND ———. 2009. Capacity of herbivorous protists to control initiation and development of mass phytoplankton blooms. *Aquat. Microb. Ecol.* **57**: 253–262, doi:10.3354/ame01358
- SMETACEK, V., R. SCHAREK, AND L. I. GORDON. 1992. Early spring phytoplankton blooms in ice platelet layers of the southern Weddell Sea, Antarctica. *Deep-Sea Res. I* **39**: 153–168.
- SMITH, C. A., AND P. SARDESHMUKH. 2000. The effect of ENSO on the intraseasonal variance of surface temperature in winter. *Int. J. Climatol.* **20**: 1543–1557, doi:10.1002/1097-0088(20001115)20:13<1543::AID-JOC579>3.0.CO;2-A
- SMITH, R. C., D. G. MARTINSON, S. E. STAMMERJOHN, R. A. IANNUZZI, AND K. IRESON. 2008. Bellingshausen and Western Antarctic Peninsula region: Pigment biomass and sea ice spatial/temporal distributions and interannual variability. *Deep-Sea Res. II* **55**: 1949–1963, doi:10.1016/j.dsr2.2008.04.027
- SPIES, A. 1987. Growth rates of Antarctic marine phytoplankton in the Weddell Sea. *Mar. Ecol. Prog. Ser.* **41**: 267–274, doi:10.3354/meps041267
- STRICKLAND, J. D. H., AND T. PARSONS. 1972. A practical handbook of sea-water analysis, 2nd ed. Fish. Res. Board Can. Bull. 167.
- SVERDRUP, H. U. 1953. On the conditions for the vernal blooming of phyto-plankton. *ICES J. Mar. Sci.* **18**: 287–295, doi:10.1093/icesjms/18.3.287
- THOMAS, M. K., C. T. KREMER, C. A. KLAUSMEIER, AND E. LITCHMAN. 2012. A global pattern of thermal adaptation in marine phytoplankton. *Science* **338**: 1085–1088, doi:10.1126/science.1224836
- TRATHAN, P. N., J. FORCADA, AND E. J. MURPHY. 2007. Environmental forcing and Southern Ocean marine predator populations: Effects of climate change and variability. *Philos. Trans. R. Soc. Lond. B* **362**: 2351–2365, doi:10.1098/rstb.2006.1953
- TURNER, J., AND OTHERS. 2005. Antarctic climate change during the last 50 years. *Int. J. Climatol.* **25**: 279–294, doi:10.1002/joc.1130
- UTERMÖHL, H. 1958. Zur Vervollkommnung der quantitativen Phytoplankton-Methodik. *Mitt. Int. Ver. Theor. Angew. Limnol.* **9**: 1–38. [For the completion of the quantitative phytoplankton methodology.]
- WALSH, J. J., D. A. DIETERLE, AND J. LENES. 2001. A numerical analysis of carbon dynamics of the Southern Ocean phytoplankton community: The roles of light and grazing in both sequestration of atmospheric CO<sub>2</sub> and food availability to larval krill. *Deep-Sea Res. I* **48**: 1–48, doi:10.1016/S0967-0637(00)00032-7
- WOOD, S. 2006. Generalized additive models: An introduction with R. Chapman and Hall/CRC.
- WRIGHT, S., R. JEFFREY, C. MANTOURA, D. LIEWELLYN, D. BJORNLAND, D. REPETA, AND N. WELSCHMEYER. 1991. Improved HPLC method for the analysis of chlorophylls and carotenoids from marine phytoplankton. *Mar. Ecol. Prog. Ser.* **77**: 183–196, doi:10.3354/meps077183
- YELLAND, M. J., AND P. K. TAYLOR. 1996. Wind stress measurements from the Open Ocean. *J. Phys. Oceanogr.* **26**: 541–558, doi:10.1175/1520-0485(1996)026<0541:WSMFTO>2.0.CO;2

Associate editor: John Albert Raven

Received: 28 January 2013

Amended: 17 September 2013

Accepted: 18 October 2013